

UC Berkeley

Working Papers

Title

A Machine Vision Based Surveillance System for California Roads

Permalink

<https://escholarship.org/uc/item/1hh5x9jw>

Authors

Malik, J.
Russell, S.

Publication Date

1995-05-01

CALIFORNIA PATH PROGRAM
INSTITUTE OF TRANSPORTATION STUDIES
UNIVERSITY OF CALIFORNIA, BERKELEY

A Machine Vision Based Surveillance System for California Roads

**J. Malik,
S. Russell**

**California PATH Research Report
UCB-ITS-PRR-95-6**

This work was performed as part of the California PATH Program of the University of California, in cooperation with the State of California Business, Transportation, and Housing Agency, Department of Transportation; and the United States Department of Transportation, Federal Highway Administration.

The contents of this report reflect the views of the authors who are responsible for the facts and the accuracy of the data presented herein. The contents do not necessarily reflect the official views or policies of the State of California. This report does not constitute a standard, specification, or regulation.

Report for MOU 83

March 1995

ISSN 1055-1425

Analysis, Design, and Evaluation of AVCS for Heavy-Duty Vehicles

Phase 1 Report

Diana Yanakiev
Ioannis Kanellakopoulos

UCLA Electrical Engineering
Los Angeles, CA 90095-1594

MOU 124

PATH Working Paper

This work was performed as part of the California PATH Program of the University of California, in cooperation with the State of California Business, Transportation, and Housing Agency, Department of Transportation; and the United States Department of Transportation, Federal Highway Administration.

The contents of this report reflect the views of the authors who are responsible for the facts and the accuracy of the data presented herein. The contents do not necessarily reflect the official views or policies of the State of California. This report does not constitute a standard, specification, or regulation.

May 1995

Analysis, Design, and Evaluation of AVCS for Heavy-Duty Vehicles — Phase 1 Report

Diana Yanakiev and Ioannis Kanellakopoulos

May 1995

Abstract

In this report we address the problem of automation of heavy-duty vehicles. After a brief description of the dynamic model used in our design and simulations, we develop nonlinear controllers with adaptation, first for speed control and then for vehicle follower longitudinal control. We consider both autonomous operation as well as intervehicle communication, and evaluate the performance of our controllers in several different scenarios through simulation.

Keywords

Adaptive Cruise Control	Control Systems
Advanced Vehicle Control Systems	Intelligent Vehicle Highway Systems
Automated Highway Systems Control	Longitudinal Control
Autonomous Intelligent Cruise Control	Public Transit
Buses	Speed Control
Commercial Vehicle Operations	Trucking
Control Algorithms	Vehicle Follower Control

Executive Summary

In the last decade, problems associated with automated highways have received a great deal of attention. While a multitude of results exists for longitudinal and lateral control of light duty vehicles, heavy-duty commercial vehicles have been largely ignored so far. These vehicles cost much more than passenger cars, are operated for profit, and spend much more time on the road. Hence, commercial vehicles may become the flagships of AVCS efforts, since the relative cost of automation is lower than in cars, while the potential financial gain is much higher. However, due to their configuration, response to braking and steering, actuator imperfections and sensitivity to winds, they cannot be controlled by simply re-tuning the controllers which have been developed for cars.

In our research funded under MOU 124, we have focused on the problem of heavy-duty vehicle automation. We have developed detailed dynamical models and designed adaptive nonlinear controllers for longitudinal control of buses and trucks. These controllers command both fuel and brake, thus eliminating the need for separate controllers and ad hoc switching logic. Furthermore, our controllers can operate in autonomous (AICC) mode but can also utilize information about the desired speed of the platoon leader in the case of intervehicle communication. Hence, they are inherently flexible and can be used in every stage of future AHS deployment.

According to the AHS Precursor Systems Analysis for Commercial Vehicles and Transit, longitudinal control of truck platoons will be one of the most challenging problems for commercial AHS. Our results to date are in complete agreement with this statement and demonstrate, as we had predicted, that longitudinal control is far more difficult for heavy trucks and buses than for passenger cars. Much more aggressive control action is needed to perform maneuvers in reasonable time. The use of nonlinear control satisfies this requirement and results in much better robustness and disturbance rejection properties than high-gain linear control. Our results also indicate that, in the case of autonomous operation, much larger time headways are required to achieve string stability in platoon formations (at least 0.7 s, compared to 0.25 s for cars). Furthermore, it appears that even with intervehicle communication it is advisable to use small time headways (0.1–0.2 sec) in order to increase safety margins and reduce fuel consumption.

Contents

- 1 Introduction** **1**

- 2 Longitudinal Truck Model** **1**
 - 2.1 Turbocharged (TC) diesel engine model 1
 - 2.2 Torque converter 4
 - 2.3 Transmission mechanicals 4
 - 2.4 Longitudinal drivetrain equations 4
 - 2.5 Linearization of the longitudinal model 6

- 3 Control Design for Speed Tracking** **6**
 - 3.1 PIQD with anti-windup 6
 - 3.2 Adaptive PIQ controller 7
 - 3.3 Comparative simulations 9

- 4 Control Design for Vehicle Following** **11**
 - 4.1 Adaptive PIQ controller 13
 - 4.2 Autonomous operation 15
 - 4.3 Intervehicle communication 15
 - 4.4 Comparative simulations 15

- 5 Conclusions** **24**

- References** **25**

List of Figures

1	Truck longitudinal model upgradable to complete lateral/longitudinal model.	2
2	TC diesel engine model representation.	3
3	Vehicle speed with PID, PIQD, adaptive PI, and adaptive PIQ control in response to a commanded staircase profile.	10
4	Performance comparison of PIQD and adaptive PIQ control.	11
5	Parameters of a truck platoon.	12
6	Autonomous operation, $h = 0$. Vehicle 1: —, 2: —, 3: —, 4: —	18
7	Autonomous operation, $h = 0.7$ s. Vehicle 1: —, 2: —, 3: —, 4: —	19
8	Autonomous operation, $h = 1.0$ s. Vehicle 1: —, 2: —, 3: —, 4: —	20
9	Intervehicle communication, $h = 0$, $k_{df} = 1$. Vehicle 1: —, 2: —, 3: —, 4: —	21
10	Intervehicle communication, $h = 0.7$ s, $k_{df} = 1$. Vehicle 1: —, 2: —, 3: —, 4: —	22
11	Intervehicle communication, $h = 1.0$ s, $k_{df} = 1$. Vehicle 1: —, 2: —, 3: —, 4: —	23

1 Introduction

Advanced Vehicle Control Systems (AVCS) are critical components of Intelligent Transportation Systems (ITS). They incorporate both longitudinal and lateral schemes for semi- or fully automated vehicle operation, aimed at increasing highway traffic flow, with improved fuel efficiency and enhanced safety. While a multitude of results exist for control of passenger cars [3, 13, 7, 17], heavy-duty commercial vehicles have been largely ignored so far. In this report we present the results of our first year of research on longitudinal control design for heavy trucks and buses.

As part of this effort we are developing realistic models which capture all the important characteristics of the longitudinal vehicle dynamics. Our first modeling task was the development of a turbocharged diesel engine model suitable for vehicle control which is briefly presented in Section 2. The engine model is then combined with the automatic transmission and drivetrain models to obtain a longitudinal heavy-duty vehicle model. The brake subsystem model is still under development; we are currently using a simplified representation adequate for longitudinal control. Section 2 also contains a linearization-based analysis of the longitudinal vehicle model, which provides useful information regarding the significance of each state for the longitudinal behavior of the vehicle. In Section 3 we develop two nonlinear control schemes for speed tracking. The performance of the designed fixed-gain PIQD and adaptive PIQ controllers is evaluated on the basis of simulation results. Existing PID and adaptive PI speed controllers are also applied to our longitudinal truck model for the sake of comparison. Then, in Section 4, we design an adaptive nonlinear controller for vehicle following which can operate in both autonomous mode (AICC) as well as in cooperative mode with intervehicle communication (platooning), and evaluate its performance under several scenarios through simulation. Finally, we present our conclusions in Section 5.

2 Longitudinal Truck Model

The longitudinal model of a truck is shown in Figure 1. The **Engine** module contains the TC diesel engine model. The four gear automatic transmission model is included in the **Transmission** block. The longitudinal dynamics equations are in the **Chassis** module.

2.1 Turbocharged (TC) diesel engine model

The vast majority of existing internal combustion engine models serves purposes such as engine performance improvement or diagnostics. Engine models meant for vehicle control have been developed only for normally aspirated spark ignition (SI) engines. Unfortunately, they cannot be adapted to describe the compression ignition (CI) of the diesel engine and to capture the effect of the turbocharger.

Using several TC diesel engine modeling techniques available in the literature [8, 16, 12, 5, 9, 6], we have compiled a model consisting of 3 differential and several algebraic equa-

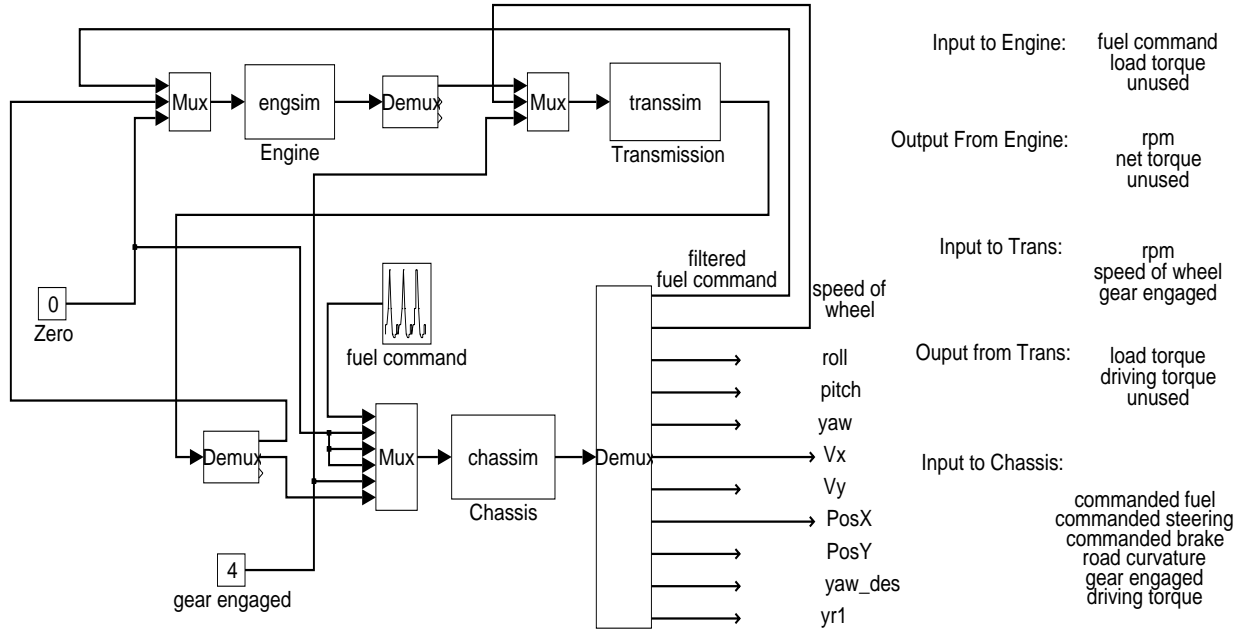


Figure 1: Truck longitudinal model upgradable to complete lateral/longitudinal model.

tions. It is based on the *mean torque production* model developed by Kao and Moskwa [10]. The modeled engine is turbocharged and intercooled, has six cylinders and 0.014 m^3 (14 liters) displacement volume. The block diagram in Figure 2 gives an overview of the model structure.

As in the SI engine model developed by Cho and Hedrick [3, 13], two of the states are the *intake manifold (IM) pressure* and the *engine speed*. However, due to the different fueling method, the fueling lag is not considered here. In the diesel engine, the fuel is injected directly into the cylinder immediately before the combustion takes place. This eliminates the need to account for the fueling dynamics. The *TC rotor speed* is another state which needs to be introduced due to the presence of the turbocharger.

The equation for the IM pressure p_{im} has been derived by differentiating the ideal gas law:

$$\dot{p}_{\text{im}} + \frac{\eta_v V_d N_e}{120 V_{\text{im}}} p_{\text{im}} = \dot{m}_c \frac{RT_{\text{im}}}{V_{\text{im}}}, \quad (2.1)$$

where T_{im} and V_{im} are respectively the IM temperature and volume, η_v is the volumetric efficiency, V_d is the displacement volume of the engine, N_e is the engine speed in revolutions per minute (rpm)—so that $N_e = \omega_e \frac{60}{2\pi}$, where ω_e is the engine speed in rad/s—and \dot{m}_c is the compressor air mass flow rate.

The engine speed ω_e is obtained by integrating the angular acceleration of the crankshaft, which is determined from Newton's second law:

$$M_{\text{ind}}(t - \tau_i) - M_f(t) - M_{\text{load}}(t) = J_e \dot{\omega}_e(t). \quad (2.2)$$

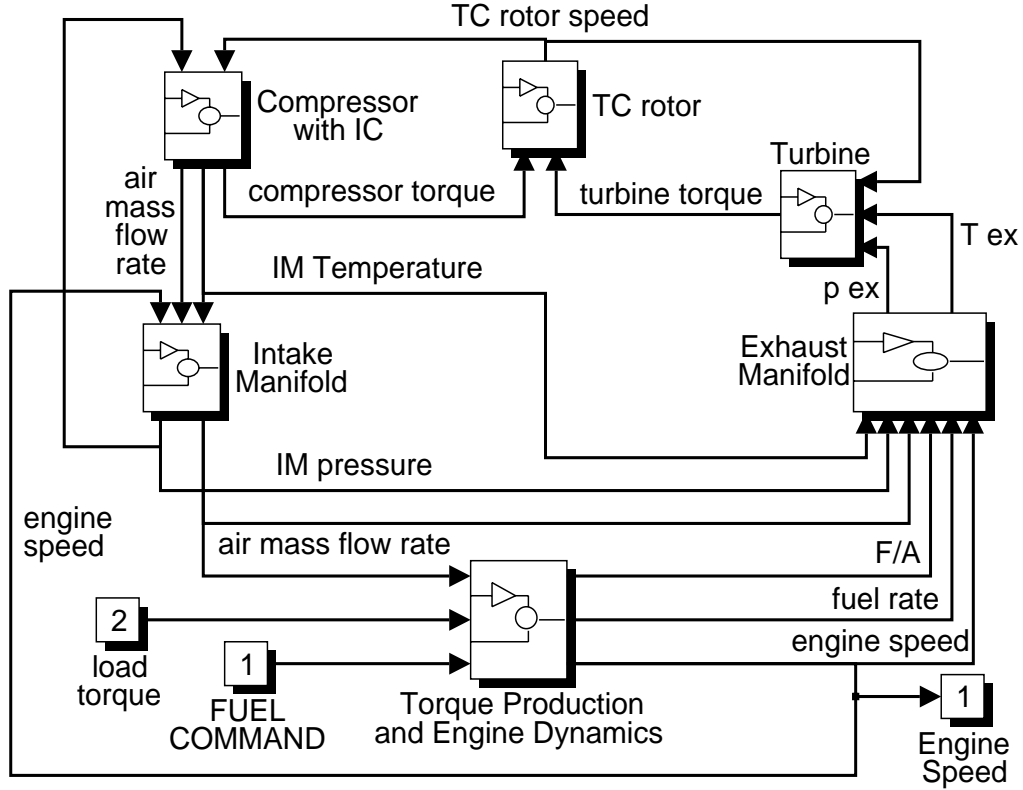


Figure 2: TC diesel engine model representation.

In the above equation, M_{ind} is the indicated torque and M_f the friction torque of the engine, M_{load} is the load torque which is determined by the transmission and the drivetrain subsystems of the vehicle model, and J_e is the effective inertia of the engine. The *production delay* τ_i represents the average difference between the time of issuing a command to change the indicated engine torque and the time when the injection valve can be operated. These events are determined by the position of the crankshaft angle. Therefore, the production delay and all other delays associated with this model have constant values measured in crankshaft angle. Converted in seconds, they become inversely proportional to the engine speed.

The TC dynamic equation is also derived using Newton's second law:

$$M_t - M_c = J_{tc} \dot{\omega}_{tc}, \quad (2.3)$$

where M_t is the torque provided by the turbine, M_c is the torque absorbed by the compressor, and J_{tc} is the effective inertia of the turbocharger. Integration of the TC angular acceleration $\dot{\omega}_{tc}$ yields the TC rotor speed ω_{tc} .

Some intermediate computations are necessary to determine the other variables participating in the state equations. Steady-state empirical characteristics and algebraic relations are used in addition to the state equations to obtain a complete mathematical description

of the system.¹

2.2 Torque converter

Our automatic transmission model is based on the assumptions that gear shifting is instantaneous and that there is no torsion in the driveline. The static nonlinear torque converter model derived by Kotwicki [11] has been employed. This model is well suited for vehicle modeling because it provides explicit terminal relations between torques and speeds. Experimentally justified approximation of the exact detailed expressions yields the following representation of the pump torque M_P and the turbine torque M_T as functions of the pump speed $\omega_P = \omega_e$ and the turbine speed ω_T :

$$M_P = \alpha_0 \omega_P^2 + \alpha_1 \omega_P \omega_T + \alpha_2 \omega_T^2 \quad (2.4)$$

$$M_T = \beta_0 \omega_P^2 + \beta_1 \omega_P \omega_T + \beta_2 \omega_T^2. \quad (2.5)$$

The coefficients $\alpha_0, \alpha_1, \alpha_2, \beta_0, \beta_1, \beta_2$ are obtained by regression from experimental data. Although the form of the equations is preserved in both modes of operation, different coefficients have to be determined for the regions when the engine is driving the vehicle and vice versa. The pump and turbine angular velocities are compared to determine the current operating region. The respective coefficients are then used to compute the pump torque, which is the load torque applied to the engine, and the turbine torque, which is the shaft torque transmitted to the drivetrain.

2.3 Transmission mechanicals

The assumption that there is no torsion in the driveline establishes a direct relationship between the angular velocity of the torque converter turbine ω_t and that of the vehicle's driving wheels ω_w :

$$\omega_w = R_{\text{total}} \omega_T = R_i R_d \omega_T, \quad (2.6)$$

where R_i is the reduction ratio of the i th gear range and R_d is the final drive reduction ratio. The model is further simplified by the instantaneous gear shifting assumption, eliminating the need for an additional state which appears during shifting.

2.4 Longitudinal drivetrain equations

The angular velocity of the driving wheels is determined by the torque converter turbine torque M_T , the tractive tire torque $F_t h_w$, where F_t is the tractive tire force and h_w is the static ground-to-axle height of the driving wheels, and the braking torque M_b :

$$J_w \dot{\omega}_w = \frac{M_T}{R_{\text{total}}} - F_t h_w - M_b, \quad (2.7)$$

¹For a detailed description of our engine and transmission model, the reader is referred to the report [18].

where J_w is the lumped inertia of the wheels.

Currently, the brake actuating system is represented via a first-order linear system with a time constant τ_b . The braking torque M_b is obtained from

$$\dot{M}_b = \frac{M_{bc} - M_b}{\tau_b}, \quad (2.8)$$

where M_{bc} is the commanded braking torque. This is a reasonable approximation for longitudinal control. We are presently developing a more elaborate brake subsystem model, which will provide the level of detail and accuracy necessary for combined lateral/longitudinal control. When completed, this subsystem will be used to generate M_b .

The tractive force F_t depends linearly on the tire slip up to approximately 15% slip. Since the tire slip is always positive, it is defined as:

$$i_d = 1 - \frac{v}{h_w \omega_w} \quad \text{or} \quad i_b = 1 - \frac{h_w \omega_w}{v}, \quad (2.9)$$

where v is the vehicle velocity, depending on whether the tire is under driving torque ($F_t = k_i i_d$) or under braking torque ($F_t = -k_i i_b$).

The aerodynamic drag force F_a and the force generated by the rolling resistance of the tires ($F_r = \frac{M_r}{h_w}$) have to be subtracted from the tractive force to yield the force that accelerates or decelerates the vehicle. The state equation for the truck velocity becomes:

$$\dot{v} = \frac{F_t - F_a - F_r}{m}, \quad (2.10)$$

where the vehicle mass is denoted by m . The force F_a is determined from the aerodynamic drag coefficient c_a and the vehicle speed:

$$F_a = c_a v^2. \quad (2.11)$$

The rolling resistance torque $M_r = F_r h_w$ is a function of the vehicle mass:

$$M_r = c_r m g. \quad (2.12)$$

Substituting (2.11) and (2.12) into (2.10), we obtain:

$$\dot{v} = \frac{F_t - c_a v^2}{m} - \frac{c_r g}{h_w}. \quad (2.13)$$

In the performed simulations the commanded index² Y is rescaled and the new input variable is denoted with u_f . The minimum index necessary to maintain idle speed corresponds to $u_f^{\min} = 3$ and the maximum index corresponds to $u_f^{\max} = 85$.

Finally, a first-order filter with a time constant τ_f is also included in the vehicle model to account for the dynamics of the fuel pump and the actuators which transmit the fuel command u to the injectors:

$$\dot{u}_f = \frac{1}{\tau_f} (-u_f + u). \quad (2.14)$$

²The index Y is defined as the position of the fuel pump rack, which determines the amount of fuel provided for combustion.

2.5 Linearization of the longitudinal model

The resulting longitudinal vehicle model described so far is highly nonlinear and detailed enough to capture all the important characteristics of the dynamic behavior of a heavy-duty vehicle. However, it is far too complex to be used as the basis for control design. It was therefore linearized around several operating points determined by different fuel command/vehicle mass combinations. The results showed that the sixth-order linearized model has the same number of dominant modes throughout the examined range, albeit with significant variations in individual parameter values. The modes associated with the angular velocity of the wheel and the fuel system (cf. (2.14)) are always very fast compared to the remaining ones, and can thus be ignored. Of the remaining four modes, those associated with the IM pressure, the engine speed and the TC rotor speed are much faster than the mode corresponding to the vehicle velocity.

Thus, the longitudinal truck model relating the vehicle speed to the fuel command input can be reduced to a first-order linear model:

$$\frac{\delta v}{\delta u} = \frac{b}{s + a}, \quad (2.15)$$

where the values of b and a depend on the operating point, i.e., on the steady state values of the vehicle speed and the load torque. This reduced-order linearized model is the basis for the design of our control schemes, which, however, are applied to and simulated with the full nonlinear model.

3 Control Design for Speed Tracking

Most longitudinal control schemes available in the literature use separate controllers for throttle and brake control. This creates the need for an additional supervisory layer, which uses *ad hoc* rules to determine which controller should be active at any given time. In contrast, our adaptive nonlinear controller is versatile enough to handle both fuel and brake, thus eliminating the undesirable overhead associated with switching logic. When the output of the controller is positive a fuel command is issued, while negative output activates the brakes. To avoid frequent switching between fuel and brake, a hysteresis element is included in the controller.

In this section we consider the problem of *speed tracking*. Two nonlinear controllers are designed: One with fixed gains and an adaptive one whose gains are continuously adjusted. Their performance is compared through simulations which use the nonlinear truck model of the previous section.

3.1 PIQD with anti-windup

We begin with the ubiquitous PID controller with an implementable approximate derivative term and an anti-windup scheme to reduce speed overshoot. In speed tracking, overshoot is

much more undesirable than undershoot because of passenger comfort considerations. It is even more undesirable in a vehicle-following scenario, where it may lead to collisions. Since overshoot is usually associated with high-gain control, one way of reducing it would be to reduce the control gains. However, this would result in longer response times. To allow fast compensation of large tracking errors without the need for high gains, we introduce a signed quadratic (Q) term into the PID controller. As we will see, our resulting nonlinear PIQD controller outperforms conventional PID controllers over a wide operating region. The PIQD control law is:

$$u = -k_p e_v - k_i \frac{1}{s} \left\{ e_v - \frac{1}{T_t} [u - \text{sat}(u)] \right\} - k_q e_v |e_v| - k_d \frac{\tau_d s}{\frac{1}{N} \tau_d s + 1} e_v, \quad (3.1)$$

where $\text{sat}(\cdot)$ is an appropriately defined saturation function that reflects the physical limits of the controller, and $e_v = v - v_d$ is the error between the actual vehicle speed v and its desired value v_d . The latter is obtained by passing the commanded speed v_c through a first-order filter to eliminate discontinuities and provide a smoother response:

$$\dot{v}_d = -v_d + v_c. \quad (3.2)$$

3.2 Adaptive PIQ controller

There are several reasons for including adaptation in our control design. Even if a controller is perfectly tuned for some operating region, it is likely to demonstrate inferior performance in other conditions due to the severe nonlinearities present in the system. A gain scheduling approach could be successful in overcoming the disadvantages of a fixed gain controller, but it would require extensive a priori information. Another reason is that adaptation makes the control design much less dependent on the specific vehicle. Keeping in mind the prospective application of AVCS to a large variety of road vehicles, the latter consideration becomes even more significant.

Let us now consider the linearized model from (2.15), where the linearization is performed around the desired speed v_d . Denoting by $e_v = v - v_d$ the deviation of the speed from its desired value v_d , we obtain the model:

$$\dot{e}_v = \dot{v} - \dot{v}_d = -a e_v + b u + d, \quad (3.3)$$

where the disturbance term d includes the external disturbances as well as the effect of the neglected fast modes.

We propose the adaptive PIQ control law:

$$u = -\hat{k}_1 e_v - \hat{k}_2 - \hat{k}_3 e_v |e_v|, \quad (3.4)$$

where \hat{k}_1 , \hat{k}_2 , \hat{k}_3 are time-varying parameters continuously adjusted by an update law. Substituting equation (3.4) into equation (3.3) yields:

$$\dot{v} = -(a + b\hat{k}_1)e_v - b\hat{k}_2 - b\hat{k}_3 e_v |e_v| + d. \quad (3.5)$$

Next, we adopt the *nonlinear* reference model:

$$\dot{v}_m - \dot{v}_d = -a_m(v_m - v_d) - q_m(v_m - v_d)|e_v|. \quad (3.6)$$

If a , b , and d were constant and known, the values of k_1 , k_2 , and k_3 satisfying the model reference control objective would be computed as

$$\begin{aligned} a + bk_1 &= a_m \\ bk_2 &= d \\ bk_3 &= q_m. \end{aligned} \quad (3.7)$$

Since the parameters of the plant are unknown, we replace k_1 , k_2 , and k_3 by their estimates in the control law (3.4). To design update laws for these estimates, we use the tracking error $e_r = v - v_m$, computed from (3.5)–(3.7) as

$$\dot{e}_r = \dot{v} - \dot{v}_m = -a_m e_r - q_m |e_v| e_r - b(\tilde{k}_1 e_v + \tilde{k}_2 + \tilde{k}_3 e_v |e_v|), \quad (3.8)$$

where $\tilde{k}_i = k_i - \hat{k}_i$, $i = 1, 2, 3$, are the parameter errors.

Instead of directly using the tracking error e_r in the update law, Xu and Ioannou [17] suggest using a *normalized estimated error* ϵ in order to improve the robustness of the adaptive controller. In the case of our nonlinear controller, this normalized error becomes

$$\epsilon = e_r - x, \quad (3.9)$$

where x is the output of the nonlinear filter:

$$\dot{x} = -a_m x - q_m |e_v| x + \epsilon e_r^2. \quad (3.10)$$

Combining (3.8), (3.9), and (3.10) we obtain:

$$\dot{\epsilon} = -a_m \epsilon - q_m |e_v| \epsilon - \epsilon_r^2 \epsilon - b(\tilde{k}_1 e_v + \tilde{k}_2 + \tilde{k}_3 e_v |e_v|). \quad (3.11)$$

Comparing (3.8) and (3.11), we see that if $e_r \gg 1$ then $\epsilon \ll e_r$, and if $e_r \ll 1$ then $\epsilon \approx e_r$. Therefore, using ϵ in the update law mitigates the effect of large tracking errors on the adaptation speed, thereby effectively reducing the bandwidth of the controller.

The update law is obtained via the partial Lyapunov function:

$$V = \frac{\epsilon^2}{2} + b \frac{\tilde{k}_1^2}{2\gamma_1} + b \frac{\tilde{k}_2^2}{2\gamma_2} + b \frac{\tilde{k}_3^2}{2\gamma_3}, \quad (3.12)$$

where γ_1 , γ_2 , γ_3 are positive design constants and b is unknown but positive. With the choices:

$$\begin{aligned} \dot{\hat{k}}_1 &= \gamma_1 \epsilon e_v \\ \dot{\hat{k}}_2 &= \gamma_2 \epsilon \\ \dot{\hat{k}}_3 &= \gamma_3 \epsilon e_v |e_v|, \end{aligned} \quad (3.13)$$

the derivative of V becomes:

$$\dot{V} = -a_m \epsilon^2 - q_m |e_v| \epsilon^2 - \epsilon_r^2 \epsilon^2. \quad (3.14)$$

This guarantees the boundedness of ϵ , \hat{k}_1 , \hat{k}_2 , \hat{k}_3 and the regulation of ϵ . Combining the boundedness and regulation of ϵ with (3.9), we see that if x is bounded and converges to zero, then so does e_r . Let us then rewrite (3.10) using $e_r = \epsilon + x$ and $e_v = e_r + v_m - v_d$:

$$\dot{x} = -a_m x - q_m x |x + \epsilon + v_m - v_d| + \epsilon(\epsilon + x)^2. \quad (3.15)$$

Since a_m and q_m are positive constants, (3.6) guarantees that $v_m - v_d$ is bounded and converges to zero. Combining this with the boundedness and convergence of ϵ , and initializing $x(0) = e_r(0)$ so that $\epsilon(0) = 0$, we conclude from (3.15) that x and, hence, e_r are bounded and converge to zero. In particular, this implies that our speed tracking objective is achieved:

$$\lim_{t \rightarrow \infty} [v(t) - v_m(t)] = 0.$$

3.3 Comparative simulations

In order to compare the performance of our two nonlinear controllers (fixed-gain PIQD and adaptive PIQ) to each other and to more conventional linear controllers (fixed-gain PID and adaptive PI), we simulated the corresponding closed-loop systems of all four controllers using the same staircase profile for the commanded vehicle speed. The comparison results between fixed-gain PID and PIQD controller, both with anti-windup, and between adaptive PI and PIQ controller are shown in Figure 3. In both cases, the inclusion of the nonlinear Q term in the control law results in better tracking of the desired speed. However, in the fixed-gain case, the improvement is more pronounced. While some overshoot is observed with the PID (despite the use of anti-windup), the PIQD overcomes this problem. Both adaptive controllers track the desired speed without overshoot. However, the performance of the adaptive PIQ controller is much more uniform for different operating conditions.

The fixed-gain PIQD and the adaptive PIQ are compared in Figure 4. The advantage of the adaptive controller is that due to adaptation it provides more uniform tracking of the desired speed over a wider range of operating conditions.

From the plotted outputs of all simulated controllers we see that aggressive control action is necessary for good tracking of step increases in the commanded speed. This confirms our intuitive expectation that more aggressive controllers are needed to overcome the considerably higher actuation-to-weight ratio of a heavy truck compared to a passenger car. However, simply increasing the gains of a linear controller would cause larger overshoot. Here we avoided this problem with the inclusion of the nonlinear Q term. Finally, we point out that the usual disadvantage of passenger discomfort due to aggressive control action is much less pronounced in heavy vehicles due to their larger mass, which results in significantly lower acceleration and jerk profiles than in passenger cars.

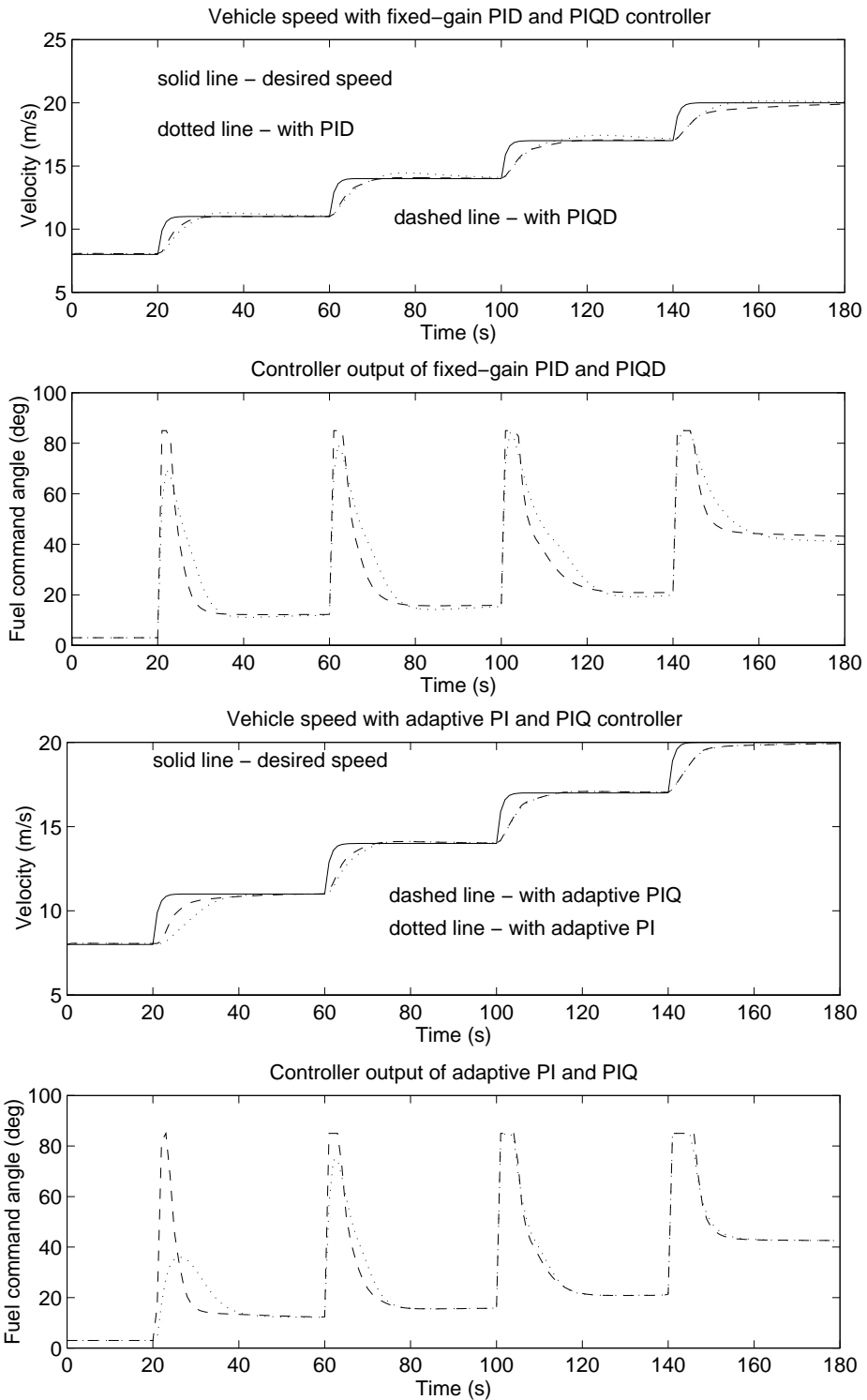


Figure 3: Vehicle speed with PID, PIQD, adaptive PI, and adaptive PIQ control in response to a commanded staircase profile.

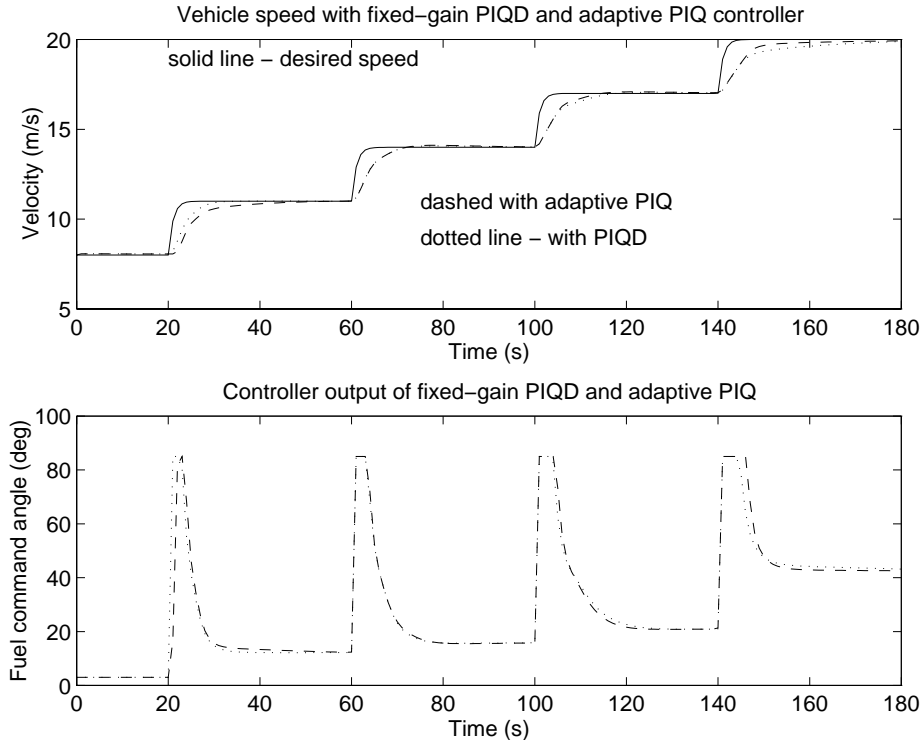
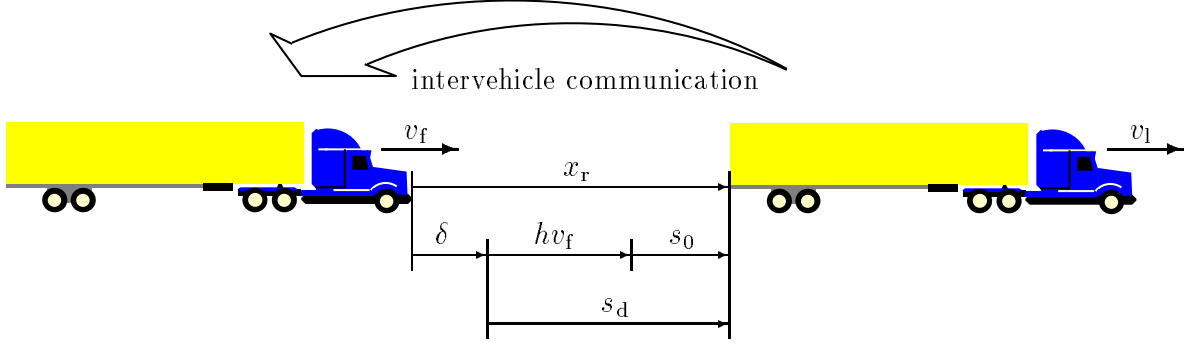


Figure 4: Performance comparison of PIQD and adaptive PIQ control.

4 Control Design for Vehicle Following

The continuous demand for increasing the traffic capacity of highway systems has so far been met by expansion of existing highways and construction of new ones. However, these solutions are quickly becoming infeasible in many large metropolitan areas. A widely proposed strategy for effectively increasing highway throughput without expansion [4, 14, 15] is to group automatically controlled vehicles in tightly spaced formations called *platoons*. Platooning provides significantly higher traffic throughput when combined with small intervehicle spacing. The control design for platoons has to guarantee not only the desired performance for individual vehicles but also for the whole formation. One of the key issues here is *string stability*, which ensures that errors decrease in magnitude as they are propagated downstream, thus eliminating the undesirable “slinky effect” associated with heavy traffic patterns. Sheikholeslam and Desoer [14] showed that string stability cannot be achieved for platoons with *constant intervehicle spacing* under autonomous operation, and proposed a scheme which guarantees string stability assuming that the lead vehicle is transmitting its velocity and acceleration information to all other vehicles in the platoon. This approach yields stable platoons with small intervehicle spacings at the cost of introducing and maintaining continuous intervehicle communication. Chien and Ioannou [2], on the other hand, proved that string stability can be recovered in autonomous operation if a *speed-dependent* spacing policy is adopted, which incorporates a *fixed time headway* term



- s_0 : minimum distance between vehicles
- h : time headway (for speed-dependent spacing)
- x_r : vehicle separation
- $s_d = s_0 + hv_f$: desired vehicle separation
- v_l : velocity of leading vehicle
- v_f : velocity of following vehicle
- $v_r = v_l - v_f$: relative vehicle velocity
- $\delta = x_r - s_d$: separation error

Figure 5: Parameters of a truck platoon.

in addition to the constant distance. Their approach avoids the communication overhead, but results in larger spacings between adjacent vehicles and thus in longer platoons, thereby yielding smaller increases in traffic throughput.

In this section we design an adaptive nonlinear controller which can operate both autonomously as well as with intervehicle communication. The quantities of interest between any two adjacent platoon members are defined in Figure 5. In the speed tracking case the primary issue addressed in the control design is regulating the difference between the actual and the desired velocity. In the vehicle-following scenario this would correspond to regulating the relative velocity $v_r = v_l - v_f$, where v_l is the leading vehicle's velocity and can be viewed as the desired speed for the following vehicle, whose actual velocity is v_f . However, in this case the controller must also regulate the separation error

$$\delta = x_r - s_d, \quad (4.1)$$

where x_r is the actual and s_d the desired separation between two adjacent vehicles. The desired separation may be a function of the following vehicle's velocity:

$$s_d = s_0 + hv_f, \quad (4.2)$$

as shown in Figure 5. The parameter h is the aforementioned *time headway* and its effect is introducing more spacing at higher velocity in addition to the *fixed minimum spacing* s_0 . Setting $h = 0$ results in a *constant spacing* policy.

The tasks of regulating the relative velocity and the separation error can be combined into the control objective $v_r + k\delta = 0$, where k is a positive design constant. This control

objective makes sense intuitively: If two vehicles are closer than desired ($\delta < 0$) but the preceding vehicle's speed is larger than the follower's ($v_r > 0$), then the controller in the following vehicle does not need to take drastic action. The same can be said if the vehicles are farther apart than desired ($\delta > 0$) but the preceding vehicle's speed is lower than the follower's ($v_r < 0$). The selection of the coefficient k influences the response of the controller, and can be changed depending on the performance requirements. Generally, a smaller k results in improved velocity tracking at the cost of deteriorated position tracking but the trend is not linear.

Let us now show that when our control objective is achieved, i.e., when $v_r + k\delta \equiv 0$, both the relative velocity and the separation error are regulated: $v_r \rightarrow 0$ and $\delta \rightarrow 0$. When the velocity of the lead vehicle is constant ($\dot{v}_l = 0$), we have

$$\delta = x_r - s_d = x_r - hv_f - s_0 \Rightarrow \dot{\delta} = v_r - h\dot{v}_f \quad (4.3)$$

$$v_r = v_l - v_f \Rightarrow \dot{v}_r = -\dot{v}_f. \quad (4.4)$$

But $v_r + k\delta \equiv 0$ implies that $\dot{v}_r + k\dot{\delta} \equiv 0$. Combining this with (4.3) and (4.4) we obtain

$$\dot{v}_r + k(v_r + h\dot{v}_r) \equiv 0 \Rightarrow (1 + kh)\dot{v}_r + kv_r \equiv 0, \quad (4.5)$$

which shows that $v_r \rightarrow 0$ (since $k > 0$ and $h > 0$). From $v_r + k\delta \equiv 0$ and $v_r \rightarrow 0$ we conclude that $\delta \rightarrow 0$.

Since the control objective is to maintain $v_r + k\delta = 0$, we linearize the model around the corresponding trajectory and obtain:

$$\dot{v}_f = a(v_r + k\delta) + bu + \bar{d}, \quad (4.6)$$

where \bar{d} incorporates external disturbances as well as modeling errors.

4.1 Adaptive PIQ controller

The platooning scenario is even more demanding than the speed tracking scenario in terms of fast response to accelerating and braking commands as well as various disturbances, and imposes even more stringent limits on overshoot. As a result, we focus on the adaptive PIQ scheme which in the speed tracking case proved to be the most successful in quickly reducing large errors without overshoot. Another argument for using adaptation in this case is that even if the grouped vehicles are not identical, they are expected to respond uniformly to different commands or disturbances. Hence, the fact that adaptation makes the controller response less dependent on the specific vehicle characteristics becomes more significant in the platoon case.

We propose the adaptive PIQ control law:

$$u = \hat{k}_1(v_r + k\delta) + \hat{k}_2 + \hat{k}_3(v_r + k\delta)|v_r + k\delta|, \quad (4.7)$$

where $\hat{k}_1, \hat{k}_2, \hat{k}_3$ are time-varying parameters which are being updated by an adaptive law. Substituting equation (4.7) into equation (4.6) yields:

$$\dot{v}_f = (a + b\hat{k}_1)(v_r + k\delta) + b\hat{k}_2 + b\hat{k}_3(v_r + k\delta)|v_r + k\delta| + \bar{d}. \quad (4.8)$$

To design update laws for the parameter estimates, we consider the nonlinear reference model:

$$\dot{v}_m = a_m(v_l - v_m + k\delta) + q_m(v_l - v_m + k\delta)|v_r + k\delta|. \quad (4.9)$$

If a, b , and \bar{d} were known, the coefficients of the controller would be computed from (3.7) with $d = -\bar{d}$. The update law for the parameter estimates is again based on the tracking error $e_r = v_f - v_m$, computed from (4.8), (4.9), and (3.7):

$$\dot{e}_r = \dot{v}_f - \dot{v}_m = -a_m e_r - q_m e_r |v_r + k\delta| + b \left[\tilde{k}_1(v_r + k\delta) + \tilde{k}_2 + \tilde{k}_3(v_r + k\delta)|v_r + k\delta| \right]. \quad (4.10)$$

Once again, in the update law we use the normalized estimated error ϵ in order to improve the robustness of the adaptive controller:

$$\epsilon = e_r - z, \quad (4.11)$$

where z is determined from:

$$\dot{z} = -a_m z - q_m |v_r + k\delta| z + \lambda(v_r^2 + \delta^2)\epsilon, \quad (4.12)$$

and λ is a small positive number. From equations (4.10)–(4.12) we obtain:

$$\dot{\epsilon} = -a_m \epsilon - q_m \epsilon |v_r + k\delta| + b(\tilde{k}_1(v_r + k\delta) + \tilde{k}_2 + \tilde{k}_3(v_r + k\delta)|v_r + k\delta|) - \lambda(v_r^2 + \delta^2)\epsilon. \quad (4.13)$$

The choices

$$\begin{aligned} \dot{\hat{k}}_1 &= -\gamma_1 \epsilon (v_r + k\delta) \\ \dot{\hat{k}}_2 &= -\gamma_2 \epsilon \\ \dot{\hat{k}}_3 &= -\gamma_3 \epsilon (v_r + k\delta) |v_r + k\delta|, \end{aligned} \quad (4.14)$$

yield the following derivative of the partial Lyapunov function (3.12):

$$\dot{V} = -a_m \epsilon^2 - q_m |v_r + k\delta| \epsilon^2 - \lambda(v_r^2 + \delta^2) \epsilon^2. \quad (4.15)$$

This guarantees the boundedness of $\epsilon, \hat{k}_1, \hat{k}_2, \hat{k}_3$ and the regulation of ϵ . An analysis similar to the speed tracking case shows that v_r and δ are also bounded and converge to zero.

4.2 Autonomous operation

As shown in the previous subsection, the presented adaptive PIQ control law guarantees individual stability of the vehicles in the platoon. Now we also need to ensure string stability, i.e., attenuation of errors as they propagate downstream.

In the case of autonomous operation, the information available to each vehicle is its own velocity and the relative velocity and separation from the preceding one. If the desired intervehicle spacing is constant, i.e., $h = 0$, string stability cannot be achieved. This result is not specific to truck platoons; similar results are available for passenger cars [14, 4, 2, 7]. This lack of stability is caused by the nature of propagating information in the platoon rather than by the particular vehicle dynamics.

A simple way to circumvent this problem without providing any additional information to the vehicles is to introduce a fixed time headway, i.e., $h > 0$ [2], thus adding time-dependent spacing to the constant spacing. This strategy is successful in achieving string stability [7] but due to the lower actuation-to-weight ratio of heavy vehicles compared to the passenger cars, the necessary minimum value of h is significantly higher. Most maneuvers require $h \geq 0.7$ s. This value yields large intervehicle spacings at higher speeds.

4.3 Intervehicle communication

If the presence of time headway which causes larger separation between adjacent vehicles is not acceptable, intervehicle communication can be introduced to obtain string stability.

Let us now consider the case where the lead vehicle transmits to all following vehicles in the platoon its desired speed v_d . This is a relatively simple scheme, which requires distinguishing only between the leader and the followers, who need not be aware of their sequential number in the platoon.

In order to incorporate the new information, the difference between the platoon leader's desired speed and the current speed of the follower is defined as $v_{df} = v_d - v_f$. The control objective is modified to $v_r + k\delta + k_{df}v_{df} = 0$, where k_{df} is a tunable parameter. If we choose $k_{df} = 0$, we recover the control objective used in the autonomous operation case.

The control law is changed to reflect the new control objective:

$$u = \hat{k}_1(v_r + k\delta + k_{df}v_{df}) + \hat{k}_2 + \hat{k}_3(v_r + k\delta + k_{df}v_{df}) |v_r + k\delta + k_{df}v_{df}|. \quad (4.16)$$

Similarly, the term $v_r + k\delta$ is replaced by $v_r + k\delta + k_{df}v_{df}$ in (4.8)–(4.15). As in the autonomous operation scenario, one can show that this control law guarantees $v_r \rightarrow 0$ and $\delta \rightarrow 0$.

The performed simulations confirm that using the above communication scheme guarantees string stability even for constant intervehicle spacing, i.e., for $h = 0$.

4.4 Comparative simulations

In order to compare the performance of the developed controller under different modes of operation, we simulated the behavior of a four-truck platoon using various scenarios.

Profiles including acceleration and deceleration commands as well as uphill and downhill grade disturbances have been examined. The commanded profile of the simulation results presented here consists of a 4 m/s step increase of the velocity at $t = 10$ s and an 8 m/s step decrease at $t = 70$ s. We chose to present the results with this profile, because they illustrate the difficulties the system might have maintaining string stability when trying to meet a challenging acceleration/deceleration objective. In all our simulation plots, the thickest lines represent the lead vehicle (Vehicle 1), while the following vehicles (Vehicles 2–4) are represented with thinner and thinner lines as their platoon position number increases.

One of the objectives of the simulation analysis is to investigate the effect of the time headway h on the platoon. When examining the simulation results, one should keep in mind that, while string stability is theoretically based on the separation error δ , the “vehicle separation” plot is practically more interesting as an indicator of string stability. The difference between the actual vehicle separation x_r and δ is best illustrated in Figure 7 where $h = 0.7$ s and x_r shows a stable trend in contrast with δ , which is slightly growing as it propagates downstream (from Vehicle 2 to Vehicle 4).

From the “vehicle separation” plots in Figures 6–8 we see that, in the autonomous operation case, string stability is achieved at the expense of a significant increase in intervehicle spacing. With $h = 0$ (Figure 6) the spacing is small, but the errors grow downstream. In fact, there is a near collision between the third and fourth vehicle at $t = 78$ s. The smallest headway for which x_r is stable is $h = 0.7$ s (Figure 7), while for $h = 1.0$ s (Figure 8) both x_r and δ are stable. These values are much larger than the $h = 0.25$ s often used for passenger cars. While it is expected that the lower actuation-to-weight ratio of heavy-duty vehicles will necessitate larger spacings than those used in car platoons, the spacings resulting from $h > 0.7$ s may be unacceptable.

If that is the case, the only currently available solution for reducing the spacing while guaranteeing string stability is the intervehicle communication scheme described in (4.16). As demonstrated in Figure 9, string stability is achieved with $h = 0$, which leads to a significant reduction in intervehicle spacing. When the time headway is increased again to $h \geq 0.7$ s, the separation errors show an unstable trend, as seen in Figures 10 and 11. This indicates that large time headways should not be used when the leader’s desired speed is transmitted, because they render the control objective used in (4.16) artificial and unreasonable. On the other hand, incorporating a small time headway ($h = 0.1 - -0.2$ s) into intervehicle communication schemes yields larger safety margins and reduced fuel consumption, since it results in less aggressive control action.

The following table shows how the simulation results in this chapter have been organized:

	$h = 0$	$h = 0.7\text{ s}$	$h = 1.0\text{ s}$
Autonomous vehicles	Figure 6 on page 18	Figure 7 on page 19	Figure 8 on page 20
Intervehicle communication	Figure 9 on page 21	Figure 10 on page 22	Figure 11 on page 23

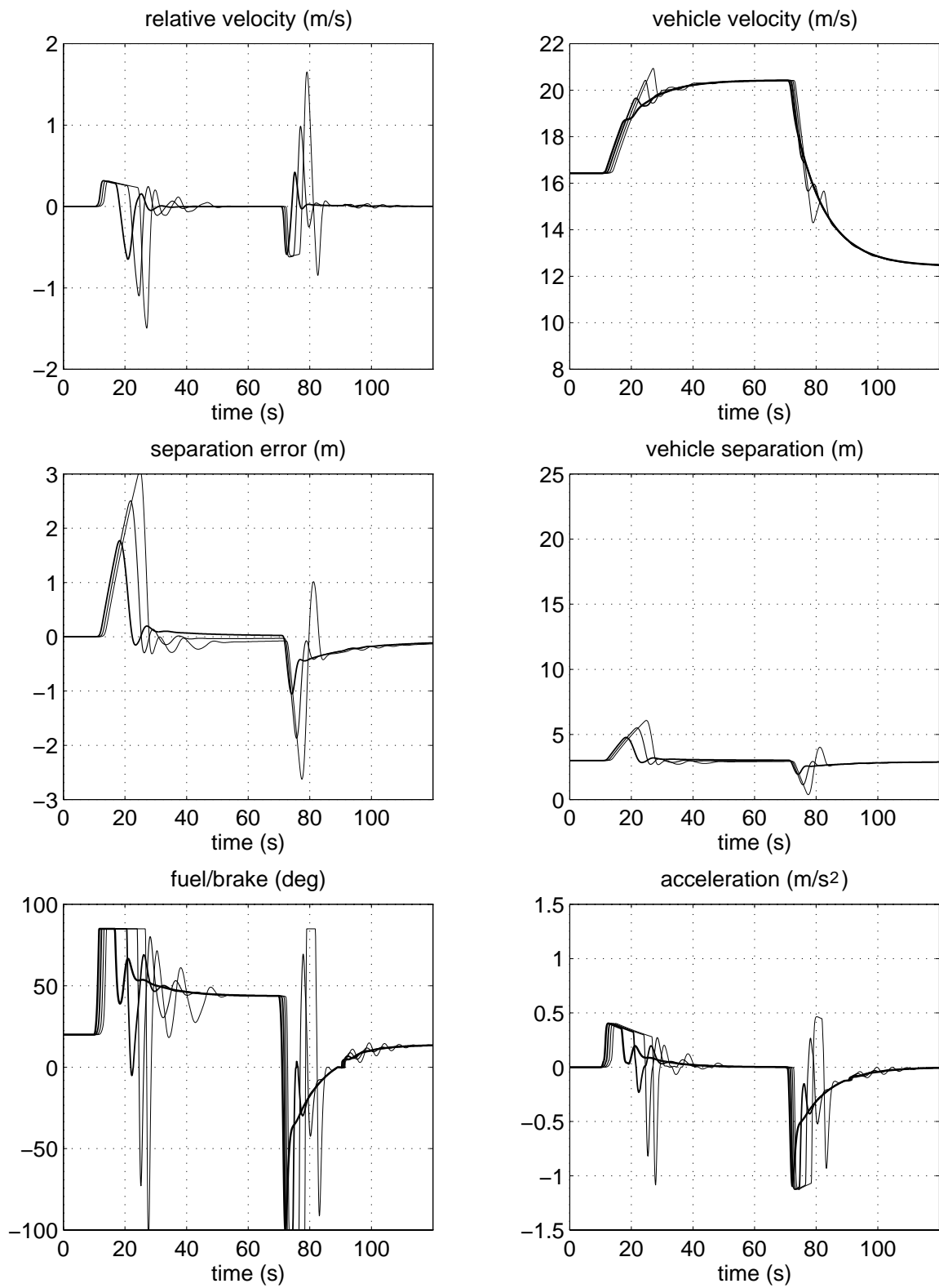


Figure 6: Autonomous operation, $h = 0$. Vehicle 1: —, 2: — —, 3: ···, 4: — ·

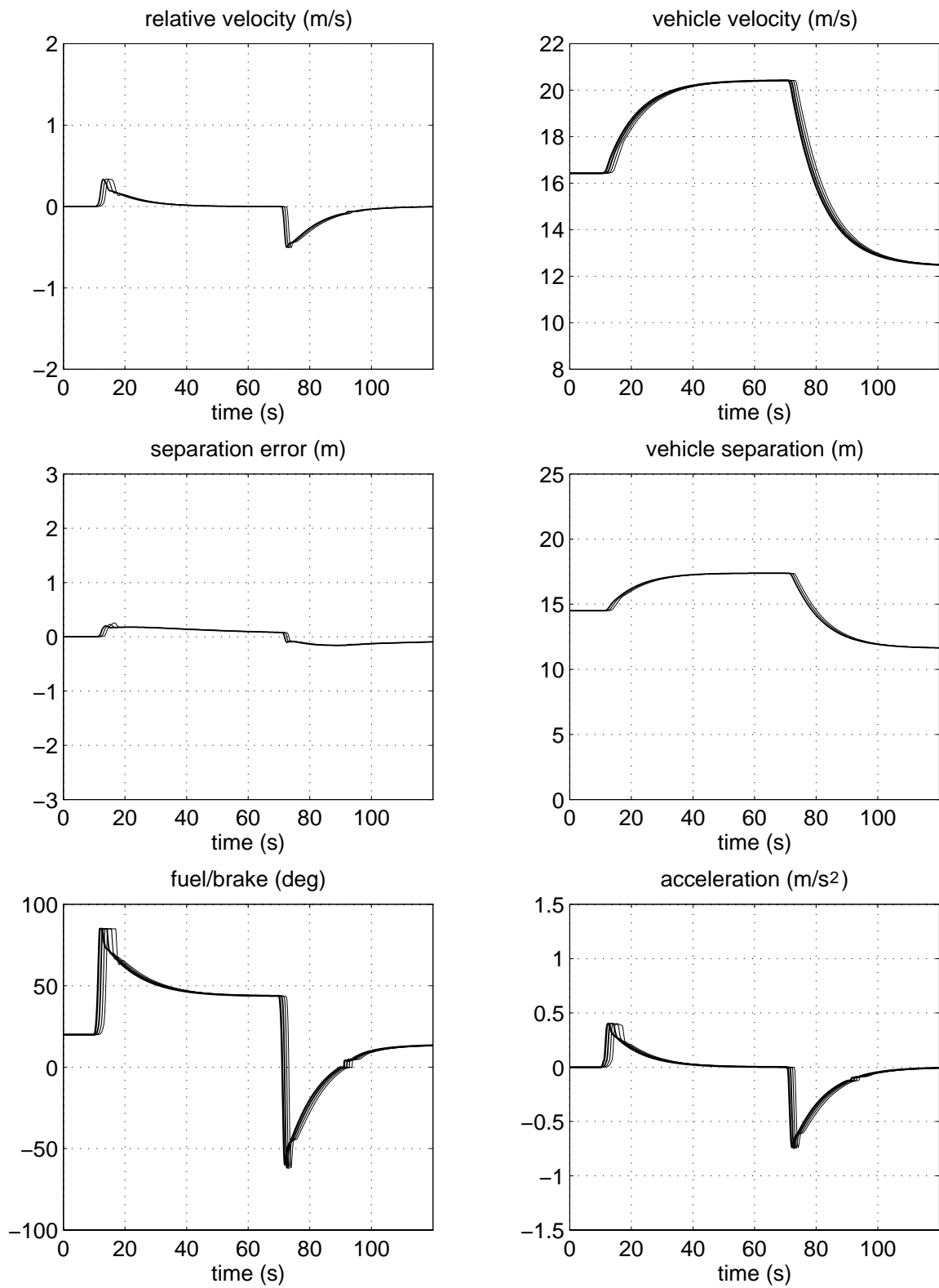


Figure 7: Autonomous operation, $h = 0.7$ s. Vehicle 1: —, 2: —, 3: —, 4: —

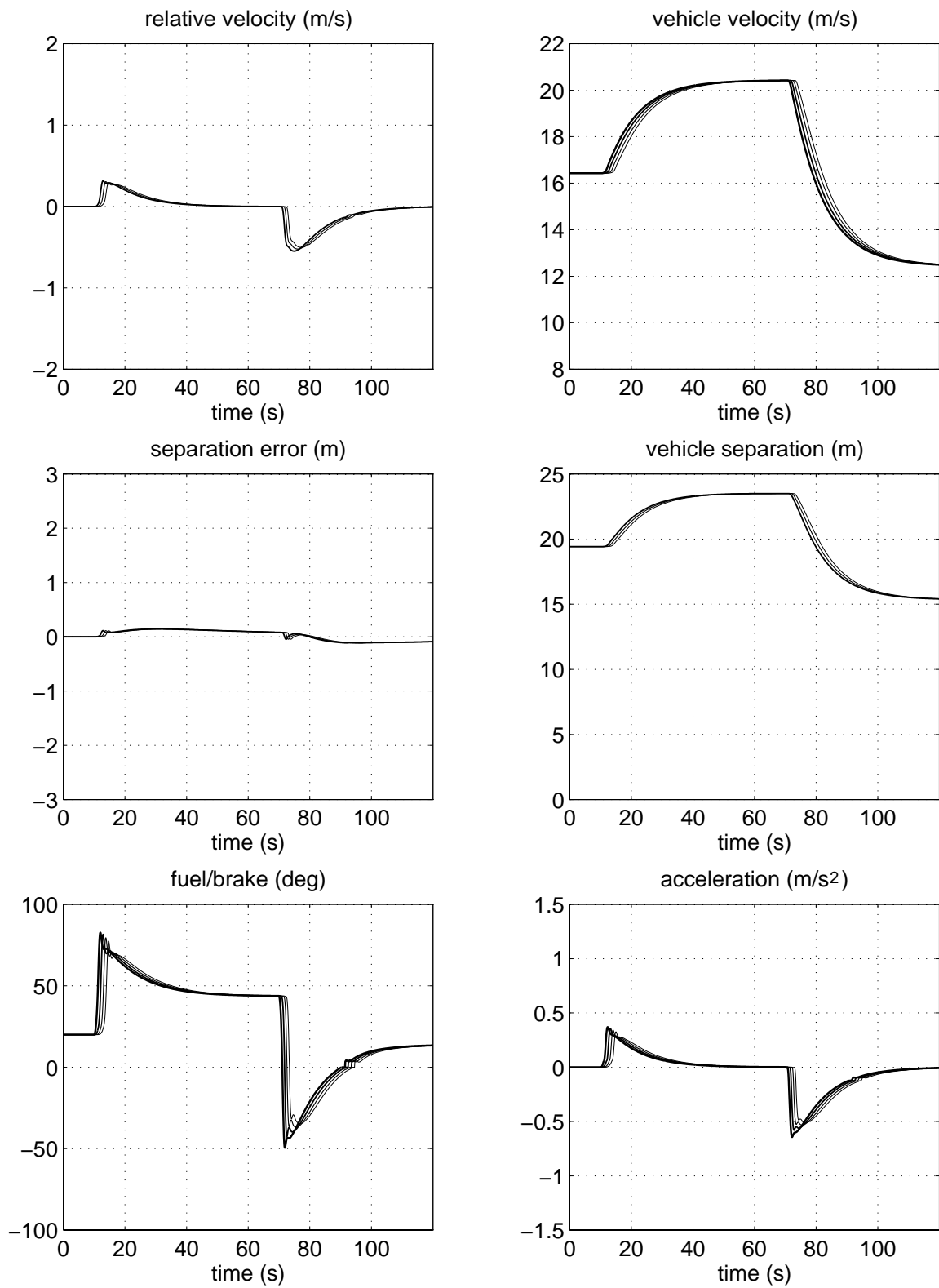


Figure 8: Autonomous operation, $h = 1.0$ s. Vehicle 1: —, 2: —, 3: —, 4: —

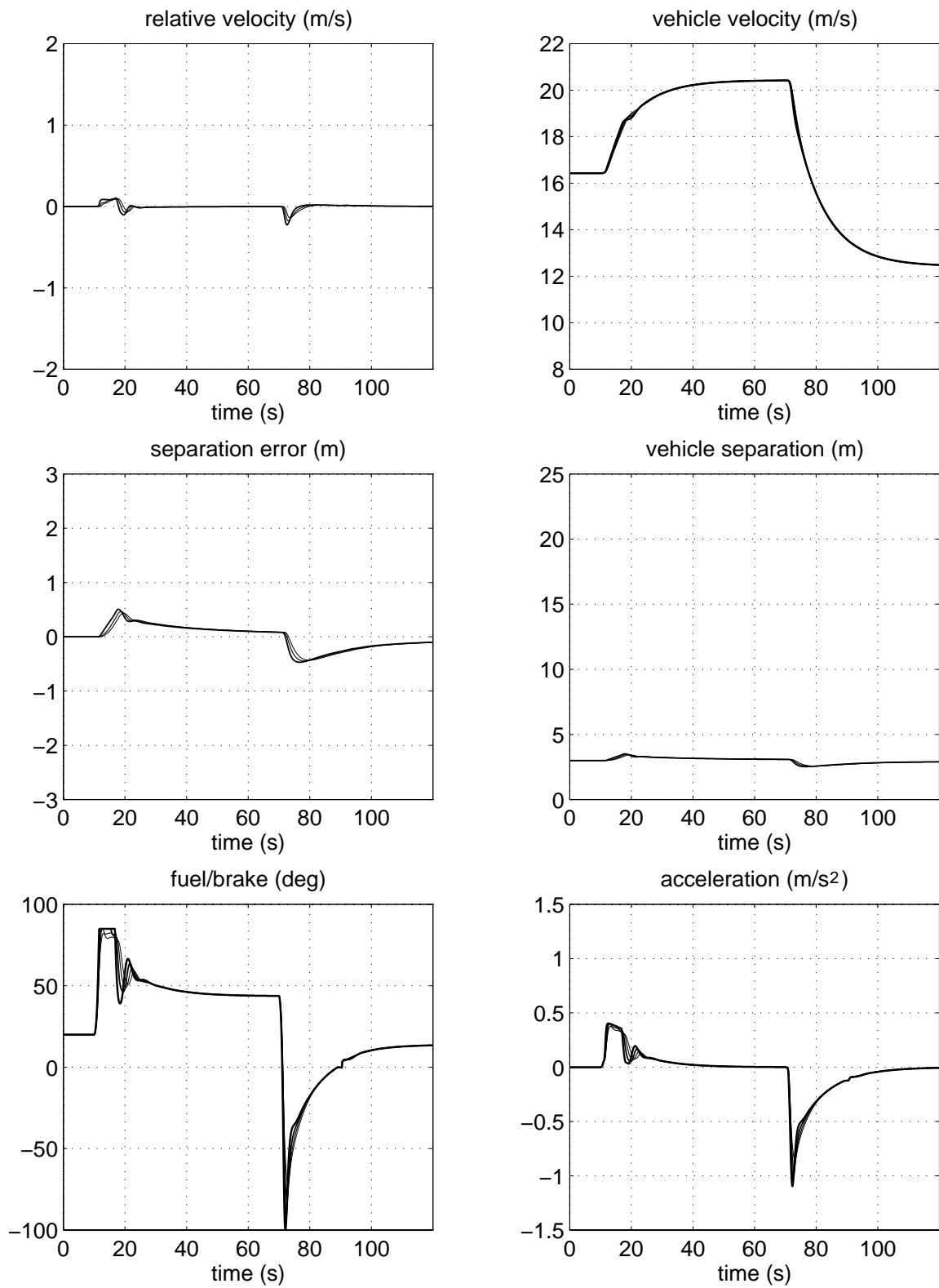


Figure 9: Intervehicle communication, $h = 0$, $k_{df} = 1$. Vehicle 1: —, 2: —, 3: —, 4: —

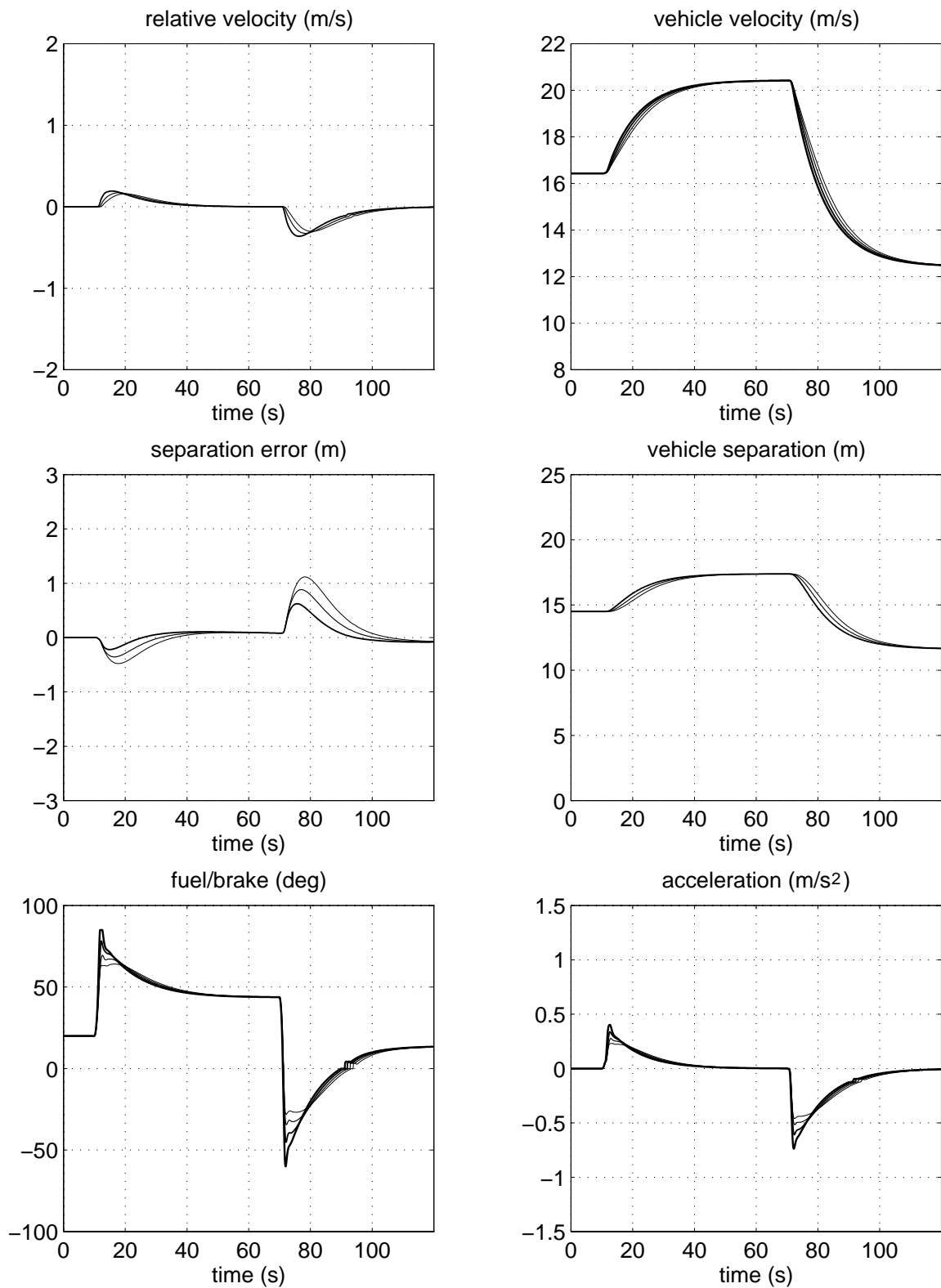


Figure 10: Intervehicle communication, $h = 0.7$ s, $k_{df} = 1$. Vehicle 1: —, 2: —, 3: —, 4: —

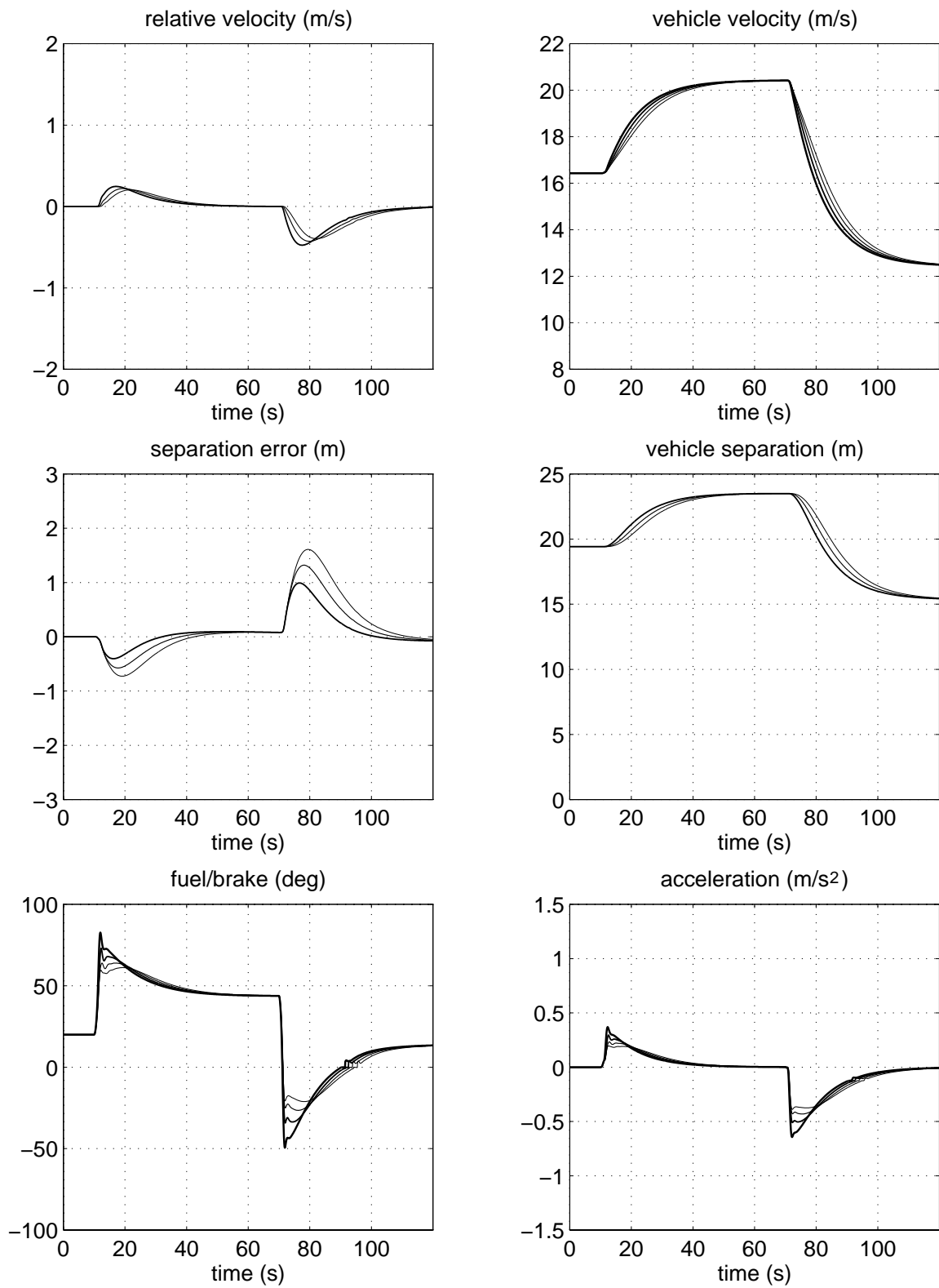


Figure 11: Intervehicle communication, $h = 1.0$ s, $k_{df} = 1$. Vehicle 1: —, 2: —, 3: —, 4: —

5 Conclusions

According to the AHS Precursor Systems Analysis for Commercial Vehicles and Transit [1], longitudinal control of truck platoons will be one of the most challenging problems for commercial AHS. Our research findings to date are in complete agreement with this statement and demonstrate, as we had predicted, that longitudinal control is much more difficult for heavy-duty vehicles than for passenger cars.

Our results confirm the intuitive expectation that more aggressive control action is needed to overcome the considerably higher actuation-to-weight ratio of a heavy bus or truck compared to a passenger car and to guarantee good performance during reasonably challenging maneuvers. The usual disadvantage of passenger discomfort due to aggressive control action is much less pronounced in heavy vehicles due to their larger mass, which results in significantly lower acceleration and jerk profiles than in passenger cars.

However, simply increasing the gains of a linear controller creates a large overshoot, which is very undesirable in vehicle following. To allow fast compensation of large errors without excessive overshoot, we include nonlinear terms in our controllers, which thus outperform conventional linear controllers. We also include adaptation to make our controller response less dependent on the specific vehicle characteristics. This results in more uniform performance over a wide operating region and across non-identical vehicles, a very desirable property in platoons.

The adaptive nonlinear controller we design commands both fuel and brake, thus eliminating the need for separate fuel and brake controllers with ad hoc switching logic. Moreover, it can operate both autonomously as well as with intervehicle communication. This flexibility is desirable for two reasons:

- A vehicle equipped with this controller can take full advantage of future automated lanes, but it can also be operated in Autonomous Intelligent Cruise Control (AICC) mode in non-automated lanes.
- The AICC capability can act as a fail-safe in automated lanes, in case there is a breakdown in intervehicle communication. In the event of such a failure, the controller can simply increase the time headway and continue to operate with guaranteed string stability, albeit with lower traffic throughput.

Our results also indicate that, in the case of autonomous operation, much larger time headways are required to achieve string stability in truck platoons—at least 0.7 s, compared to 0.25 s for cars. Furthermore, it appears that even with intervehicle communication, small time headways (0.1–0.2 s) result in increased safety margins and less aggressive control action, hence in reduced fuel consumption.

References

- [1] F. Bottiger, H. D. Chemnitz, J. Doorman, U. Franke, T. Zimmermann, and Z. Zomotor, “Commercial vehicle and transit AHS analysis,” *Precursor Systems Analyses of Automated Highway Systems*, Final Report, vol. 6, Federal Highway Administration, Report FHWA-RD-95-XXX, 1995.
- [2] C. Chien and P. Ioannou, “Automatic vehicle following,” *Proc. 1992 American Control Conf.*, Chicago, IL, pp. 1748–1752.
- [3] D. Cho and J. K. Hedrick, “Automotive power train modeling for control,” *Transactions of ASME*, vol. 111, pp. 568–576, 1989.
- [4] J. K. Hedrick, D. H. McMahon, V. K. Narendran, and D. Swaroop, “Longitudinal vehicle controller design for IVHS systems,” *Proc. 1991 American Control Conf.*, Boston, MA, pp. 3107–3112.
- [5] E. Hendricks, “Mean value modeling of large turbocharged two-stroke diesel engine,” *SAE Transactions*, paper no. 890564, pp. 1–10, 1989.
- [6] J. H. Horlock and D. E. Winterbone, *The Thermodynamics and Gas Dynamics of Internal Combustion Engines*, Clarendon Press, Oxford, 1986.
- [7] P. Ioannou and Z. Xu, “Throttle and brake control systems for automatic vehicle following,” *IVHS Journal*, vol. 1, pp. 345–377, 1994.
- [8] M. J. Jennings, P. N. Blumberg, and R. W. Amann, “A dynamic simulation of Detroit diesel electronic control system in heavy duty truck powertrains,” *SAE Transactions*, paper no. 861959, pp. 5.943–5.966, 1986.
- [9] J. P. Jensen, A. F. Kristensen, S. C. Sorenson, and E. Hendricks, “Mean value modeling of a small turbocharged diesel engine,” *SAE Transactions*, paper no. 910070, pp. 1–13, 1991.
- [10] M. Kao and J. J. Moskwa, “Turbocharged diesel engine modeling for nonlinear engine control and state estimation,” *Proceedings of the 1993 ASME Winter Annual Meeting*, DSC-vol. 52, Symposium on Advanced Automotive Technologies: Advanced Engine Control Systems, New Orleans, LA.
- [11] A. J. Kotwicki, “Dynamic models for torque converter equipped vehicles,” *SAE Transactions*, paper no. 820393, pp. 1595–1609, 1982.
- [12] J. D. Ledger, R. S. Benson, and N. D. Whitehouse, “Dynamic modeling of a turbocharged diesel engine,” *SAE Transactions*, paper no. 710177, pp. 1–12, 1971.
- [13] D. H. McMahon, J. K. Hedrick, and S. E. Shladover, “Vehicle modeling and control for automated highway system,” *Proceedings of the 1990 American Control Conference*, San Diego, CA, pp. 297–303.

- [14] S. Sheikholeslam and C. A. Desoer, “Longitudinal control of a platoon of vehicles,” *Proc. 1990 American Control Conf.*, San Diego, CA, pp. 291–297.
- [15] P. Varaiya, “Smart cars on smart roads: problems of control,” *IEEE Trans. Automatic Control*, vol. 38, pp. 195–207, 1993.
- [16] D. E. Winterbone, C. Thiruarooran, and P. E. Wellstead, “A wholly dynamic model of turbocharged diesel engine for transfer function evaluation,” *SAE Transactions*, paper no. 770124, pp. 1–11, 1977.
- [17] Z. Xu and P. Ioannou, “Adaptive throttle control for speed tracking,” *Vehicle System Dynamics*, vol. 23, pp. 293–306, 1994.
- [18] D. Yanakiev and I. Kanellakopoulos, “Engine and transmission modeling for heavy-duty vehicles,” University of California, Los Angeles, California PATH Program, PATH Technical Note, to appear, May 1995.